

Original article

DOI: <https://doi.org/10.18721/JPM.16407>

## SIZE EFFECTS IN MOLECULAR DYNAMICS SIMULATIONS OF A FULLERENE ION IMPACT ON THE SILICON SURFACE

*K. P. Karasev<sup>1,2</sup>✉, S. D. Strizhkin<sup>1</sup>, P. A. Karaseov<sup>1</sup>, A. I. Titov<sup>1</sup>*

<sup>1</sup> Peter the Great St. Petersburg Polytechnic University, St. Petersburg, Russia;

<sup>2</sup> Alferov University of RAS, St. Petersburg, Russia

✉ [kir.karasyov2017@yandex.ru](mailto:kir.karasyov2017@yandex.ru)

**Abstract.** In the paper, the interaction of an accelerated  $C_{60}$  fullerene ion with silicon monocrystal surface has been studied using molecular dynamics simulation. The dependence of a resulting crater size and sputtering yield on the initial size of the target was obtained. We proposed that computational artifacts revealed in simulations appeared due to two main reasons: shock waves raised by impinging the  $C_{60}$  ion, came back through the periodic boundary increasing the temperature around the impact point; dissipation of the energy, brought to the surface by the fullerene molecule, between small amount of atoms in the small cell might also affect the simulated results. It was established that  $11 \times 11$  nm is the least size of lateral crystal dimensions required for the valid results of the simulation of the 8–14 keV  $C_{60}$  ion impact.

**Keywords:** molecular dynamics simulation,  $C_{60}$  fullerene ion, silicon, size effect, crystal, sputtering

**Funding:** The reported study was carried out within the framework of the State Assignment for Fundamental Research (Subject Code FSEG-2023-0016).

**Citation:** Karasev K. P., Strizhkin S. D., Karaseov P. A., Titov A. I., Size effects in molecular dynamics simulations of a fullerene ion impact on the silicon surface, St. Petersburg State Polytechnical University Journal. Physics and Mathematics. 16 (4) (2023) 76–85. DOI: <https://doi.org/10.18721/JPM.16407>

This is an open access article under the CC BY-NC 4.0 license (<https://creativecommons.org/licenses/by-nc/4.0/>)



Научная статья  
УДК 539.21  
DOI: <https://doi.org/10.18721/JPM.16407>

## РАЗМЕРНЫЕ ЭФФЕКТЫ ПРИ МОЛЕКУЛЯРНО-ДИНАМИЧЕСКОМ МОДЕЛИРОВАНИИ ПАДЕНИЯ ИОНА ФУЛЛЕРЕНА НА ПОВЕРХНОСТЬ КРЕМНИЯ

К. П. Карасев<sup>1,2</sup>✉, Д. А. Стрижкин<sup>1</sup>, П. А. Карасев<sup>1</sup>, А. И. Титов<sup>1</sup>

<sup>1</sup> Санкт-Петербургский политехнический университет Петра Великого,  
Санкт-Петербург, Россия;

<sup>2</sup> Академический университет им. Ж. И. Алфёрова РАН, Санкт-Петербург, Россия  
✉ [kir.karasyov2017@yandex.ru](mailto:kir.karasyov2017@yandex.ru)

**Аннотация.** В работе выполнено моделирование взаимодействия ускоренных ионов фуллерена  $C_{60}$  с монокристаллом кремния. Исследовано влияние размеров модельного монокристалла на получаемые параметры кратера, образующегося в мишени при ударе, и распыление веществ мишени и фуллерена. Предлагаются причины возникновения вычислительных артефактов: это возврат энергии ударной волны через периодическую границу и не вполне корректное описание распределения принесенной энергии между атомами мишени. Установлено, что для получения достоверных (без размерных эффектов) результатов моделирования акта падения на монокристалл ионов  $C_{60}$ , обладающих энергиями 8 – 14 кэВ, необходимо использовать монокристаллы с размерами поверхности не менее  $11 \times 11$  нм.

**Ключевые слова:** молекулярно-динамическое моделирование, ион фуллерена  $C_{60}$ , кремний, размерный эффект, кристалл, распыление

**Финансирование:** Работа выполнена в рамках Государственного задания на проведение фундаментальных исследований (код темы FSEG-2023-0016).

**Ссылка для цитирования:** Карасев К. П., Стрижкин Д. А., Карасев П. А., Титов А. И. Размерные эффекты при молекулярно-динамическом моделировании падения иона фуллерена на поверхность кремния // Научно-технические ведомости СПбГПУ. Физико-математические науки. 2023. Т. 4 № .16. С. 76–85. DOI: <https://doi.org/10.18721/JPM.16407>

Статья открытого доступа, распространяемая по лицензии CC BY-NC 4.0 (<https://creativecommons.org/licenses/by-nc/4.0/>)

### Introduction

Molecular dynamics (MD) simulation is widely used in modern science to study various phenomena at the micro level. It consists in simulating the time evolution of a system of objects (atoms), calculated by numerical integration of equations of motion. The motion of a particle ensemble can be uniquely given by a Hamiltonian in the classical-mechanics approximation, determined by a set of generalized coordinates and momenta. This Hamiltonian characterizes the total energy of the system and fully describes its dynamic nature. The MD method can be applied to analyze both simple crystal structures and complex biological molecules [1]. The MD method is also often used to study the effects occurring under irradiation of various targets with accelerated ions. Studies based on MD simulation established the mechanisms behind the evolution of structural defects [2] and the relief of the target surface [3] under ion bombardment. In particular, the dependences of the mass transfer function and the surface morphology on the initial beam incidence angle were determined [3]. Additionally, numerous papers focused on sputtering of ions incident on the surface: the number and composition of outgoing particles, their angular distribution over incident energies of bombarding ions [4].

Simulations are generally aimed at determining the forces with which particles interact with each other, since their values are necessary to calculate the atomic coordinates and momenta at subsequent points in time. The resulting force depends on the interaction potential and the spatial configuration of the particles and is calculated for each point in time.

Many functions have been developed to describe the interaction between particles, for example, the Lennard–Jones pairwise potential [5], allowing to calculate the force of interaction between two atoms depending on the distance between them. This is often used to simulate two-dimensional structures such as graphene or transition metal dichalcogenides. However, pairwise potentials do not take into account the dependence of the binding force on the directions and positions of neighboring particles in space, which narrows the scope of their applicability. For this reason, multiparticle potentials have been developed, in particular, the Tersoff potential [6] and Stillinger–Weber potential [7]. These potentials adequately describe the properties of silicon single crystals at certain parameter values, so they are often used in calculations.

An important aspect to be taken into account in MD simulations is the limited size of the system under consideration, which means it is nearly impossible to model the behavior of macroscopic objects by this approach. For example, beam diameter in experiments on bombardment of the surface with fullerene ions [8] ranged from 0.1 to 5 mm, while the sizes of the irradiated samples were even larger. The exposure times range from tens of seconds to several hours. However, simulating the motion of such a large number of atoms requires too much computing power, so only models with tens or hundreds of thousands of atoms have to be used. Periodic boundary conditions are imposed on the sides of the target, while thermostatic conditions are additionally imposed on the motion of external atomic layers in the crystal to match the model to the real sample, allowing to regulate heat flows, further reducing the computational time.

Earlier studies [9] found that a crater appears in the region around the cluster ion's impact point, with a small cluster of atoms forming above the surface along the crater's edge, known as its rim. In addition, was found that  $C_{60}$  ions impinging on the surface of a single silicon crystal completely destroy the cluster structure if their initial energy exceeds 1 keV [10]. Carbon atoms penetrate deep into the target and are distributed in a certain way, while some of the particles escape from the surface. Such particles are called sputtered and can consist of both single atoms and their agglomerates, i.e., clusters.

As an accelerated ion impinges on the surface, its energy is transferred to the target atoms, while part of it (especially in the case of molecules or clusters consisting of dozens or more atoms) can propagate deep into the crystal as a shock wave. As noted above, the dimensions of the cell used in calculations significantly affect the computing power and time. On the other hand, propagation of a shock wave in a small crystal model and the dissipation of the energy brought by an ion in this model may differ significantly from those in a real target. Accordingly, the simulation will give incorrect values for the effects obtained, such as sputtering, crater formation, etc.

This paper compares the single cases of  $C_{60}$  fullerene ions with energies of 8 and 14 keV impinging on the surface of silicon single crystals with different sizes, analyzing the influence of these sizes on the results.

Recommendations were formulated based on the data obtained for choosing the optimal dimensions of the computational cell for modeling the interaction of accelerated fullerene molecules with a silicon single crystal.

### Description of the model

The open-source Lammmps package was used to run the MD simulations [11]. Pairwise interaction of all types of atoms was described by the Tersoff potential [6], smoothly splined to the ZBL potential to describe the interaction of high-energy particles [12]. The initial system consisted of a silicon crystal with the (100) open surface, with a  $C_{60}$  fullerene molecule located at some height above it.

Periodic boundary conditions were imposed in the lateral directions; the three lower atomic layers were fixed. A Berendsen thermostat [13] consisting of a layer of silicon atoms with a thickness of one unit cell was used on the sides and bottom of the crystal.

The target temperature was approximately 0 K. The energy losses of fast particles due to interaction with target electrons (electron losses) were taken into account as a quasi-friction force applied to particles with energies over 10 eV. Several configurations of the lateral dimensions of the target (in nm) were considered:



$5.4 \times 5.4$ ;  $8.0 \times 8.0$ ;  $11.0 \times 11.0$ ;  $22 \times 22$ ;  $33 \times 33$ ;  $44 \times 44$ ,

which adequately corresponds to the values (in the unit cell lengths)

$10 \times 10$ ,  $15 \times 15$ ,  $20 \times 20$ ,  $40 \times 40$ ,  $60 \times 60$ ,  $80 \times 80$ .

The target thicknesses were taken to be 11, 17 and 34 nm, i.e., 20, 31 and 63 in edge lengths of the unit cell; the edge length of the silicon unit cell is 0.543 nm.

All atoms of the  $C_{60}$  molecule were given the same velocity in the normal direction to the target surface at the initial time instant. The incident energy of fullerene amounted to 8 and 14 keV, and the initial temperature of the silicon crystal was 0 K. A variable time step was used to increase the computational accuracy at the initial stage as well as to speed up calculations after the particle energy decreased sufficiently.

The highest value of the time step was 1 fs. The total simulation time was selected depending on the initial fullerene energy: specifically, it was 5 and 10 ps for 8 and 14 keV, respectively. After the simulation was completed, the structures formed on the surface and the parameters of the sputtered particles were analyzed by the techniques described in [14]. Next, the system was restored to its initial state: the fullerene molecule was moved to a small random distance in the lateral directions (within  $2 \times 2$  unit cells) and the calculation of a new trajectory began. For each combination of crystal size and  $C_{60}$  ion energy, 50 independent trajectories were calculated to reduce the statistical spread of the results.

### Results and discussion

As mentioned in the introduction, MD simulations are performed for crystals with small sizes and periodic boundary conditions. Adding a thermostat along the boundary layers provides dissipation of excess energy brought to the target by an accelerated ion. At the same time, if the crystal size is too small, various computational artifacts may appear (i.e., results that do not reflect the real processes), therefore, it is necessary to avoid such phenomena as much as possible. We performed a series of calculations for molecules with energies of 8 and 14 keV impinging on silicon crystals of various sizes.

Fig. 1 shows how the appearance of a 1 nm thick cross section changes in the region where 8 keV fullerene impinges on it with an increase in the lateral size of the target. Here, the depth of the model crystal was 17 nm in all cases (31 is the length of the silicon unit cell). Evidently, the shape of the crater changes with increasing size in the lateral directions: it becomes wider and more spherical. Furthermore, it is highly likely that the volume of the amorphized target region changes to some extent.

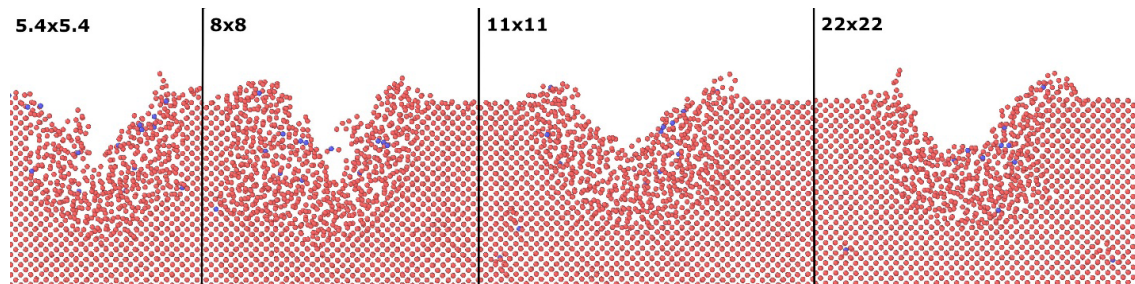


Fig. 1. Cross sections of a region of 10 Å thick silicon target after impact from 8 keV  $C_{60}$  fullerene ion with an energy (4 cases of lateral dimensions of the target (in nm))

Let us consider the changes in the shape of the crater in more detail, using the techniques for determining its volume, depth and opening area proposed in [14]. Fig. 2,*a* shows the dependence of the volume of the formed crater on the lateral dimensions of the model crystal at a constant thickness of 17 nm. It is clear that the volume of the crater increased by about 2 times at both energies, with an increase in the model size from 5.43 to 21.70 nm (from 10 to 40 unit cells). This effect turns out to be even more pronounced if the crater's opening area is increased, determined



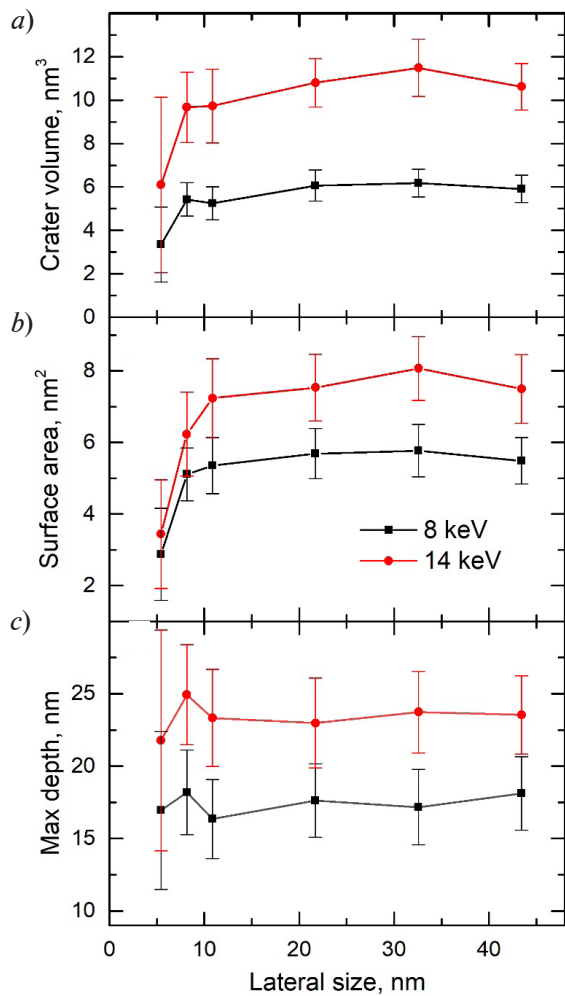


Fig. 2. Dependences of volume (a), surface area (b) and maximum depth (c) of the crater formed in a silicon target with a depth of 17 nm on its lateral dimensions. The results are given for the  $C_{60}$  ion energies of 8 and 14 keV

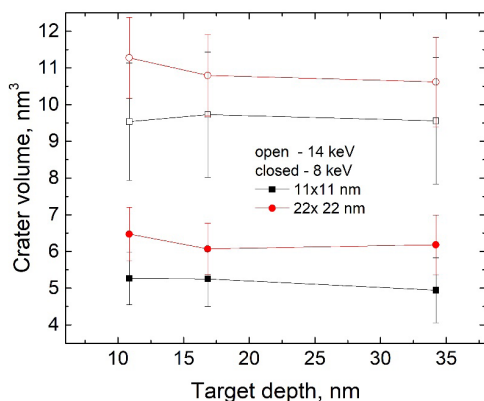


Fig. 3. Calculated dependences of mean volume of crater formed by impinging 8 and 14 keV fullerene ions on the depth of the model target with lateral dimensions of the crystal equal to  $11 \times 11$  and  $22 \times 22$  nm

at the level of the initial surface of the target [14]. The area varies from 3.0 to 5.5 nm<sup>2</sup> in the case of bombardment with fullerene at an energy of 8 keV, and from 3.5 to 8.0 nm<sup>2</sup> in the case of bombardment with fullerene at an energy of 14 keV. On the other hand, increasing the lateral dimensions of the model to  $20 \times 20$  nm or more practically does not affect the formation of the crater (see Fig. 2). We should note (see Fig. 2,c) that the maximum depth of the crater practically does not depend on the lateral dimensions of the target used.

In addition to the lateral dimensions, the thickness of the target layer considered can also play a major role. To clarify this issue, we performed a series of calculations with different model depths given that the lateral dimensions of the crystal were equal to  $11 \times 11$  and  $22 \times 22$  nm. The obtained volumes of the crater are shown in Fig. 3. Apparently, a decrease in depth from 17 to 11 nm leads to some changes in the values of the obtained volumes, while its increase to 34 nm does not affect the results in any way. The opening area of the crater and its depth also practically do not depend on the thickness of the calculated model in the considered range. Thus, the lateral dimensions of the model used in the simulation of impinging fullerenes at energies of 8–14 keV play a more significant role in the formation of possible computational artifacts than its thickness, if the latter exceeds 10–15 nm.

As mentioned above, as a fullerene ion impinges on the target, some of the silicon atoms gain kinetic energy sufficient to overcome the forces of interatomic attraction and escape from the surface as sputtered particles. It is obvious that the dimensions of the calculated model can strongly influence the sputtering characteristics obtained as a result of the simulated effect.

Fig. 4,a shows the obtained dependences of the total number of sputtered atoms and the number of backscattered carbon atoms on the lateral dimensions of the target. Evidently, increasing them from  $5 \times 5$  to  $11 \times 11$  nm in the lateral dimensions leads to a decrease in the total number of escaping particles by about 2 times. The number of backscattered carbon atoms changes even more noticeably. Indeed, the calculation with the smallest cell yields 12–13 sputtered carbon atoms and depends on the energy of incident fullerene. This number decreases to 6–7 for a cell with a size of  $11 \times 11$  nm. A further increase in the lateral dimensions of the crystal does not affect the resulting sputtering.

Analyzing the angular distributions of the sputtered particles, we can observe a similar

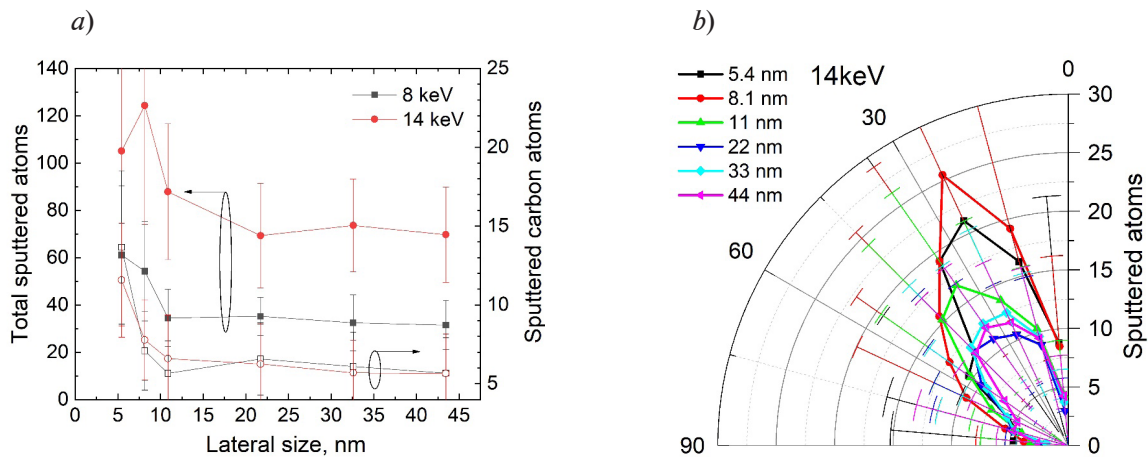


Fig. 4. Dependence of the total number of sputtered particles and backscattered carbon atoms on the lateral dimensions of the target (a); angular distributions of sputtered atoms for different lateral dimensions of the crystal with a depth of 17 nm. Cases of impact from  $C_{60}$  fullerene ions at energies of 8 and 14 keV (a) as well as 14 keV (b) are shown.

trend (Fig. 4,b). The distribution has a pronounced maximum in the direction of  $25^\circ$  from the normal for a crystal with a small surface area. As the size increases, the distribution becomes more symmetrical, and the maximum shifts towards  $35\text{--}40^\circ$ . A further increase in the size of the cell in the range of 22–44 nm does not lead to a change in the resulting distribution.

Notably, the magnitude of the statistical spread in the obtained values of both total and differential sputtering yields is significantly reduced for targets of  $22 \times 22$  nm and larger. The variation in the depth of the model crystal practically does not affect either the absolute number of sputtered particles or their distributions.

To understand the causes behind the discovered computational artifacts, we analyzed the propagation of shock waves occurring in the target. Fig. 5 shows the characteristic patterns obtained by MD simulation, which can occur during interaction in models with a depth of 17 nm at different lateral dimensions.

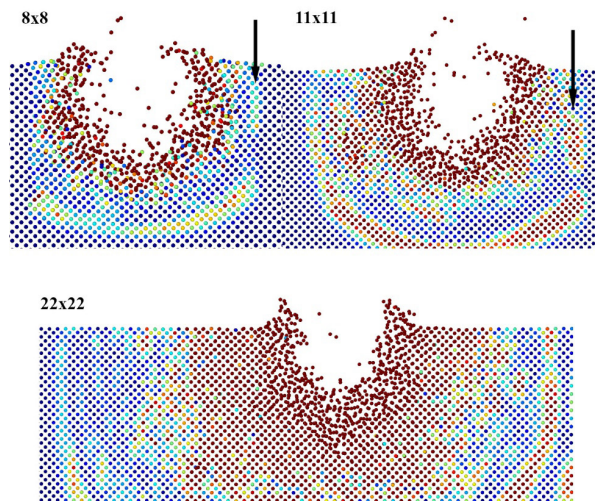


Fig. 5. Characteristic views of cross section (thickness 10 E) of model with the depth of 17 nm, evolving in the interaction of the fullerene ion with the target at three different lateral dimensions of the target (in nm). The colors of the atoms (small circles) correspond to different kinetic energies (see Table); the arrows indicate the segments of waves passing through the periodic boundary and propagating to the region where the crater forms.

Table

**Parameters of target atoms (see Fig. 5)**

Lateral size of target, nm	Kinetic energy of silicon atoms, eV	Time period, ps
$8 \times 8 \times 17$	0–0.20	0.4
$11 \times 11 \times 17$	0–0.05	0.5
$22 \times 22 \times 17$	0–0.01	1.1

Notes. 1. The time intervals between the instants when the  $C_{60}$  ion impinges on the surface and the patterns shown in Fig. 5 are recorded.

2. The  $C_{60}$  ion had an energy of 8 keV.

The arrows in the two upper patterns (see Fig. 5, models with sizes of  $8 \times 8$  and  $11 \times 11$  nm) show the segments of waves passing through the periodic boundary and propagating towards the region where the crater formed rather than away from it. Such a phenomenon could not be detected in the case of simulation with a  $22 \times 22$  nm cell: all visible waves propagated from the impact point and attenuated near the thermostat.

The table shows the time instants at which the images were taken and the energy ranges used to conveniently describe the wave processes in different cases. We should note that the energies of silicon atoms reach 0.20 and 0.05 eV in cells with the dimensions of  $8 \times 8$  and  $11 \times 11$  nm, respectively, i.e., the calculated temperatures near the crater exceed 900 K. All atoms have an energy of less than 0.01 eV in a  $22 \times 22$  nm cell. Thus, the energy transferred by the fullerene ion does not have time to dissipate into the target volume at small cell sizes and returns to the impact area through periodic boundaries; this leads to increased relaxation of produced defects and a decrease in the size of the crater by maintaining an elevated temperature for a longer time than in the case of larger model crystals. The effect of the return shock wave may also be associated with increased sputtering, including in directions closer to the normal. In the case of large cells, the scattering and dissipation of the energy transferred between atoms are more uniform and better correspond to the picture observed experimentally.

### Conclusion

The paper presents a molecular dynamics simulation of the interaction between the  $C_{60}$  fullerene ions, with energies of 8 and 14 keV, and the surface of a silicon single crystal. In particular, we considered the influence of the size of this single crystal on the results obtained.

We found that various computational artifacts arise at an energy of 8 keV and lateral dimensions of less than  $11 \times 11$  nm, both as a crater evolves in the target and during sputtering of particles caused by its bombardment. Varying the depth of the model crystal in the range from 11 to 33 nm had practically no effect on the results obtained. The cell dimensions of  $11 \times 11$  nm turned out to be insufficient at the incident energy of 14 keV, since slightly overestimated sputtering yields are produced in this case, although no artifacts were observed during the formation of the crater.

It was established that the causes of the artifacts were, firstly, the return of energy transferred by fullerene through periodic boundaries to the region where the crater formed, and secondly, somewhat incorrectly calculated distribution of the energy transferred between the target atoms in the case of small models.

Analyzing our findings, we can conclude that a model with the dimensions of  $11 \times 11$  nm is preferable for simulating the interaction of  $C_{60}$  ions at a kinetic energy of less than 8 keV with the target; it is recommended to use cells with larger lateral dimensions for the case of 14 keV.



## REFERENCES

1. **Arnittali M., Rissanou A. N., Amprazi M., et al.**, Structure and thermal stability of wtRop and RM6 proteins through all-atom molecular dynamics simulations and experiments, *Int. J. Mol. Sci.* 22 (11) (2021) 5931.
2. **Ullah M. W., Kuronen A., Nordlund K., et al.**, Atomistic simulation of damage production by atomic and molecular ion irradiation in GaN, *J. Appl. Phys.* 112 (4) (2012) 043517.
3. **Maciążek D., Kański M., Postawa Z.**, Intuitive model of surface modification induced by cluster ion beams, *Anal. Chem.* 92 (10) (2020) 7349–7353.
4. **Aoki T., Matsuo J.**, Molecular dynamics study of surface modification with a glancing angle gas cluster ion beam, *Nucl. Instrum. Methods Phys. Res. B.* 255 (1) (2007) 265–268.
5. **Lennard-Jones J. E.**, On the determination of molecular fields. – II. From the equation of state of a gas, *Proc. R. Soc. Lond.* 106 (738) (1924) 463–477.
6. **Tersoff J.**, New empirical approach for the structure and energy of covalent systems, *Phys. Rev. B.* 37 (12) (1988) 6991–7000.
7. **Stillinger F. H., Weber T. A.**, Computer simulation of local order in condensed phases of silicon, *Phys. Rev. B.* 31 (8) (1985) 5262–5271.
8. **Khadem M., Pukha V., Penkov O., et al.**, Formation of wear-resistant graphite/diamond-like carbon nanocomposite coatings on Ti using accelerated C<sub>60</sub>-ions, *Surf. Coat. Technol.* 424 (25 Oct) (2021) 127670.
9. **Aoki T., Seki T., Matsuo J.**, Molecular dynamics simulations for gas cluster ion beam processes, *Vacuum.* 84 (8) (2010) 994–998.
10. **Skripov I. N., Karasev K. P., Strizhkin D. A., Karasev P. A.**, Issledovaniye poverkhnostnykh yavleniy pri padenii uskorennoogo iona C<sub>60</sub> na monokristall kremniya [Study of surface phenomena in the impact of an accelerated C<sub>60</sub> ion on a Si monocrystal], In book of abstracts: Proceedings of All-Russian Conference “Scientific week at Institute of Electronics and Telecommunications of St. Petersburg Polytechnical University”, Nov. 15–19 2021, SPb. (2021) 55–57 (in Russian).
11. **Thompson A. P., Aktulga H. M., Berger R., et al.**, LAMMPS – a flexible simulation tool for particle-based materials modeling at the atomic, meso, and continuum scales, *Comp. Phys. Commun.* 271 (Febr) (2022) 108171.
12. **Ziegler J. F., Biersack J. P., Littmark U.**, The stopping and range of ions in matter (Book series: Stopping and range of ions in matter. Vol. 1), Pergamon, New York, 1985.
13. **Berendsen H. J. C., Postma J. P. M., van Gunsteren W. F., et al.**, Molecular dynamics with coupling to an external bath, *J. Chem. Phys.* 81 (8) (1984) 3684–3690.
14. **Karasev K., Strizhkin D., Karasev P.**, The way to analyze MD simulation results of cluster ion bombardment, *IEEE Xplore Proc. 2023 Int. Conf. Electric. Eng. Photon. (EExPolytech-2023)*, Oct. 19–20 2023, St. Petersburg, SPbPU, (2023) 282–284.

## СПИСОК ЛИТЕРАТУРЫ

1. **Arnittali M., Rissanou A. N., Amprazi M., Kokkinidis M., Harmandaris V.** Structure and thermal stability of wtRop and RM6 proteins through all-atom molecular dynamics simulations and experiments // *International Journal of Molecular Sciences*. 2021. Vol. 22. No. 11. P. 5931.
2. **Ullah M. W., Kuronen A., Nordlund K., Djurabekova F., Karasev P. A., Titov A. I.** Atomistic simulation of damage production by atomic and molecular ion irradiation in GaN // *Journal of Applied Physics*. 2012. Vol. 112. No. 4. P. 043517.
3. **Maciążek D., Kański M., Postawa Z.** Intuitive model of surface modification induced by cluster ion beams // *Analytical Chemistry*. 2020. Vol. 92. No. 10. Pp. 7349–7353.
4. **Aoki T., Matsuo J.** Molecular dynamics study of surface modification with a glancing angle gas cluster ion beam // *Nuclear Instruments and Methods in Physics Research. B.* 2007. Vol. 255. No. 1. Pp. 265–268.
5. **Lennard-Jones J. E.** On the determination of molecular fields. II. From the equation of state of a gas // *Proceedings of the Royal Society A, London*. 1924. Vol. 106. No. 738. Pp. 463–477.
6. **Tersoff J.** New empirical approach for the structure and energy of covalent systems // *Physical Review B*. 1988. Vol. 37. No. 12. Pp. 6991–7000.



7. **Stillinger F. H., Weber T. A.** Computer simulation of local order in condensed phases of silicon // *Physical Review B*. 1985. Vol. 31. No. 8. Pp. 5262–5271.
8. **Khadem M., Pukha V., Penkov O., Khodos I., Belmesov A., Nechaev G., Kabachkov E., Karaseov P., Kim D.-E.** Formation of wear-resistant graphite/diamond-like carbon nanocomposite coatings on Ti using accelerated  $C_{60}$ -ions // *Surface and Coatings Technology*. 2021. Vol. 424. 25 October. P. 127670.
9. **Aoki T., Seki T., Matsuo J.** Molecular dynamics simulations for gas cluster ion beam processes // *Vacuum*. 2010. Vol. 84. No. 8. Pp. 994–998.
10. **Скрипов И. Н., Карасев К. П., Стрижкин Д. А., Карасев П. А.** Исследование поверхностных явлений при падении ускоренного иона  $C_{60}$  на монокристалл кремния // Неделя науки ИЭиТ (Институт электроники и телекоммуникаций). Материалы Всероссийской конференции. СПб., СПбПУ. 15–19 ноября 2021. С. 55–57.
11. **Thompson A. P., Aktulga H. M., Berger R., et al.** LAMMPS – a flexible simulation tool for particle-based materials modeling at the atomic, meso, and continuum scales // *Computer Physics Communications*. 2022. Vol. 271. February. P. 108171.
12. **Ziegler J. F., Biersack J. P., Littmark U.** The stopping and range of ions in matter (Book series: Stopping and range of ions in matter. Vol. 1). New York: Pergamon, 1985. 321 p.
13. **Berendsen H. J. C., Postma J. P. M., van Gunsteren W. F., DiNola A., Haak J. R.** Molecular dynamics with coupling to an external bath // *The Journal of Chemical Physics*. 1984. Vol. 81. No. 8. Pp. 3684–3690.
14. **Karasev K., Strizhkin D., Karaseov P.** The way to analyze MD simulation results of cluster ion bombardment // *IEEE Xplore Proceedings of the 2023 International Conference on Electrical Engineering and Photonics (EExPolytech-2023)*. St. Petersburg, SPbPU, October 19–20, 2023. Pp. 282–284.

## THE AUTHORS

### **KARASEV Kirill P.**

*Peter the Great St. Petersburg Polytechnic University,  
Alferov University of RAS*  
29 Politechnicheskaya St., St. Petersburg, 195251, Russia  
kir.karasyov2017@yandex.ru  
ORCID: 0000-0002-0969-0162

### **STRIZHKIN Denis A.**

*Peter the Great St. Petersburg Polytechnic University*  
29 Politechnicheskaya St., St. Petersburg, 195251, Russia  
strdenis02@gmail.com  
ORCID: 0009-0003-1062-8360

### **KARASEOV Platon A.**

*Peter the Great St. Petersburg Polytechnic University*  
29 Politechnicheskaya St., St. Petersburg, 195251, Russia  
platon.karaseov@spbstu.ru  
ORCID: 0000-0003-2511-0188

### **TITOV Andrei I.**

*Peter the Great St. Petersburg Polytechnic University*  
29 Politechnicheskaya St., St. Petersburg, 195251, Russia  
andrei.titov@rphf.spbstu.ru  
ORCID: 0000-0003-4933-9534

**СВЕДЕНИЯ ОБ АВТОРАХ**

**КАРАСЕВ Кирилл Платонович** – инженер-исследователь Высшей инженерно-физической школы Санкт-Петербургского политехнического университета Петра Великого, студент Академического университета им. Ж. И. Алфёрова РАН.

195251, Россия, г. Санкт-Петербург, Политехническая ул., 29

kir.karasyov2017@yandex.ru

ORCID: 0000-0002-0969-0162

**СТРИЖКИН Денис Александрович** – лаборант-исследователь Высшей инженерно-физической школы Санкт-Петербургского политехнического университета Петра Великого.

195251, Россия, г. Санкт-Петербург, Политехническая ул., 29

strdenis02@gmail.com

ORCID: 0009-0003-1062-8360

**КАРАСЕВ Платон Александрович** – доктор физико-математических наук, профессор Высшей инженерно-физической школы Санкт-Петербургского политехнического университета Петра Великого.

195251, Россия, г. Санкт-Петербург, Политехническая ул., 29

platon.karaseov@spbstu.ru

ORCID: 0000-0003-2511-0188

**ТИТОВ Андрей Иванович** – доктор физико-математических наук, профессор Высшей инженерно-физической школы Санкт-Петербургского политехнического университета Петра Великого.

195251, Россия, г. Санкт-Петербург, Политехническая ул., 29

andrei.titov@rphf.spbstu.ru

ORCID: 0000-0003-4933-9534

*Received 01.12.2023. Approved after reviewing 04.12.2023. Accepted 04.12.2023.*

*Статья поступила в редакцию 01.12.2023. Одобрена после рецензирования 04.12.2023. Принята 04.12.2023.*